J. Fluid Mech. (1991), *vol.* 227, *pp.* 393–406
Printed in Great Britain

Elliptical vortices and integrable Hamiltonian dynamics of the rotating shallow-water equations†

By DARRYL D. HOLM
Theoretical Division and Center for Nonlinear Studies, Los Alamos National Laboratory, MS B284, Los Alamos, NM 87545, USA

(Received 30 May 1990)

The problem of the dynamics of elliptical-vortex solutions of the rotating shallow-water equations is solved in Lagrangian coordinates using methods of Hamiltonian mechanics. All such solutions are shown to be quasi-periodic by reducing the problem to quadratures in terms of physically meaningful variables. All of the relative equilibria – including the well-known rodon solution – are shown to be orbitally Lyapunov stable to perturbations in the class of elliptical-vortex solutions.

1. Introduction

Goldsbrough (1930) observed that the shallow-water equations in a rotating frame admit exact elliptical-vortex solutions, whose velocity components are linear and whose height function is quadratic in the Eulerian coordinates, with coefficients depending on time. These lens-shaped solutions – with uniform vorticity, elliptically shaped flowlines, and parabolic height profiles – are the analogues for the rotating shallow-water (RSW) equations of the Kirchhoff (1876) vortex for the two-dimensional Euler equations (in which the velocity components are linear in the coordinates and the *pressure* is quadratic). Inclusion of the height function for the RSW elliptic-vortex solutions introduces an additional degree of freedom beyond that of the Kirchhoff vortex, leading to slightly richer dynamics.

The 12-dimensional system of nonlinear coupled ordinary differential equations for elliptical-vortex RSW dynamics have been investigated by various authors, leading to a sequence of increasingly more complete solutions with applications to tidal oscillations, warm-core rings, and other upper-ocean phenomena. Ball (1963) uses the integral properties of the RSW equations to decouple the centre-of-mass motion and an axisymmetric pulsation from the rest of the elliptical-vortex motion, thereby reducing the problem to an eight-dimensional dynamical system. Using this system, Ball (1965) and Thacker (1981) investigate tidal oscillations in elliptical basins whose depth profile is parabolic. Oscillations and rotations of warm-core rings are studied by Cushman-Roisin, Heil & Nof (1985) and Cushman-Roisin (1987), who find a periodically pulsating axisymmetric solution and a steadily rotating elliptical solution of the eight-dimensional-vortex system. The latter is a uniformly rotating ellipse of constant shape (i.e. eccentricity) and size (i.e. area), which has been called the 'rodon'. Ripa (1987) studies Lyapunov stability of the 'circular rodon' (i.e. a circular, uniformly rotating RSW vortex) finding them stable to disturbances in the class of elliptic solutions and unstable to higher-order polynomial disturbances.

Young (1986) uses the theorems of Ball (1963) and the invariants of the RSW equations to reduce the eighth-order elliptical-vortex dynamics to quadratures,

† With an Appendix by D. David and T. K. Ohsumi.

thereby proving that the elliptic-vortex solution is in general quasi-periodic, not chaotic. The analysis in the Eulerian description is tortuous, however, involving several substitutions and transformations of variables, and resulting in quadratures from which the full solution is complicated to reconstruct. Rogers & Ames (1989) discuss Ball's theorems on the motion of the centre of mass and on the oscillation of the moment of inertia using the framework of invariance group analysis for the shallow-water equations. In that framework they show that the particular solutions obtained by Thacker (1981) are group-invariant solutions. Rogers (1989) derives additional group-invariant vortex solutions. The elliptical-vortex solutions are also studied numerically in Kirwan & Liu (1991).

These authors all work in Eulerian coordinates, while we work in the Lagrangian description. The Lagrangian description has a familiar particle-dynamics character and admits a canonical (symplectic) Hamiltonian formulation. (The Hamiltonian structure of the RSW equations in Eulerian coordinates is Lie–Poisson, see Holm & Long (1989) and references therein.) We show that elliptical-vortex motion reduces in the Lagrangian description to one-degree-of-freedom classical Hamiltonian mechanics, which may be investigated fully. The constants of motion are analogous to the usual angular momentum conservation law implied by rotational symmetry, and the dynamics of the reduced system is periodic. Hence, the dynamics of the full system is quasi-periodic, and hardly more complex than harmonic motion superposed upon precession.

An early use of Lagrangian coordinates to derive exact solutions of Euler's equations describing fluid flow with linear velocity profiles in three dimensions appears in Greenhill (1879), for circulation of a fluid of constant density within an ellipsoidal cavity. Even before Greenhill, fluid flows with linear profiles had been studied in Lagrangian coordinates by Dirichlet (1860), Dedekind (1860), and Riemann (1860), in connection with ellipsoidal figures of equilibrium for self-gravitating incompressible fluid masses. The history and development of the latter topic is given with extensive references by Chandrasekhar (1969). Rotating ellipsoidal-vortex solutions for incompressible fluids with linear velocity profiles are also treated in the classical texts by Basset (1880) and Lamb (1932). Lagrangian techniques for studying ellipsoidal-vortex solutions with linear velocity profiles are used in Dyson (1968) for ideal compressible fluids, in Holm (1982, 1983) for ideal compressible magnetohydrodynamics, and in Holm (1986) for stratified Boussinesq fluids. In each of these cases, the dynamics turns out to be analogous to gyroscopic motion.

The plan of the present paper is as follows. Section 2 discusses the RSW equations and the elliptical-vortex solution Ansatz in both Eulerian and Lagrangian coordinates. Section 3 gives the action principle and Hamiltonian formulation of elliptical-vortex dynamics in the Lagrangian description, as well as the constants of motion implied by the continuous symmetries of the Hamiltonian. A discrete symmetry under interchange of Eulerian and Lagrangian coordinates is also identified. This discrete symmetry implies a principle of duality, first formulated explicitly by Dedekind (1860) in discussing the dynamics of an incompressible fluid ellipsoid held together by gravitation. Applying the Dedekind duality principle to elliptical-vortex solutions of the RSW equations interchanges the angular momentum of the elliptical-vortex with its (integrated) potential vorticity; thereby relating, for example, uniformly rotating solutions having no potential vorticity to their dual solutions having potential vorticity but no angular momentum. Section 4 uses the method of Hamiltonian reduction and Ball's (1963) theorem on the simple harmonic oscillations of the moment of inertia for RSW solutions to reduce the elliptical-vortex problem to Newtonian single-particle dynamics for the aspect ratio of the ellipse, solvable by quadrature in the usual way from a first integral. The known solutions of axisymmetric pulsation, uniform steady rotation (the rodon), and a combined motion of steady rotation and periodic pulsation (the so-called pulsrodon), as well as their dual solutions, are all recovered as simple special cases of the complete solution.

2. The shallow-water equations in a rotating frame

The shallow-water equations in a rotating planar domain are (summing on repeated indices and using subscript-comma notation for spatial derivatives)

$$\frac{\partial v_i}{\partial t} = (\omega+f)\,\epsilon_{ij}\,v^j - (\tfrac{1}{2}v^2+gh)_{,i}, \quad i,j = 1,2, \tag{2.1}$$

$$\frac{\partial h}{\partial t} = -(hv^i)_{,i}. \tag{2.2}$$

Here the constants f and g denote the Coriolis parameter and reduced gravity, respectively. The other notation is

$$v^2 = v_i v^i, \quad \omega = \epsilon_{ij}\,v^j_{,i}, \quad i,j = 1,2; \quad \epsilon = \begin{pmatrix} 0 & 1 \\ -1 & 0 \end{pmatrix}. \tag{2.3}$$

The horizontal velocity components, v_i, $i = 1,2$, and the height function h of the fluid depend on the two Eulerian spatial dimensions (x_1, x_2) plus time, t:

$$v_i = (v_1(x_1,x_2,t), v_2(x_1,x_2,t)), \quad h = h(x_1,x_2,t). \tag{2.4}$$

Goldsbrough's (1930) elliptical-vortex solution Ansatz for these equations is that the fluid velocity $\boldsymbol{v}$ is linear in the Eulerian coordinates $\boldsymbol{x} = (x_1, x_2)$ in the plane, and the surface height (or depth) h is quadratic in these coordinates. That is,

$$\boldsymbol{v}(\boldsymbol{x},t) = \boldsymbol{A}(t)\cdot\boldsymbol{x}, \quad h(\boldsymbol{x},t) = h_0(t) - \boldsymbol{x}^{\mathrm{T}}\cdot\boldsymbol{B}(t)\cdot\boldsymbol{x}, \tag{2.5}$$

where $\boldsymbol{A}(t)$ and $\boldsymbol{B}(t)$ are 2×2 matrices depending only on time, and $\boldsymbol{B}$ is symmetric and positive definite. The units of $\boldsymbol{A}$ and $\boldsymbol{B}$ are inverse time and inverse length, respectively. The solution Ansatz (2.5) represents a swirling, rotating fluid mass in the shape of a horizontally truncated ellipsoid. Its upper boundary is the flat, horizontal ellipse at $h = 0$. Substitution of this Ansatz into the shallow-water equations leads to a closed system of eight ordinary differential equations for $h_0(t)$, $\boldsymbol{A}(t)$, and $\boldsymbol{B}(t)$, which have been rather extensively studied as discussed in the introduction. Here we seek to simplify these ordinary differential equations by first recasting the problem as a canonical Hamiltonian system in different, Lagrangian, variables. In these variables, two of the four degrees of freedom fall into action-angle pairs. These action-angle pairs for the elliptical vortex are: first, angular momentum and its canonically conjugate angle, the orientation of the ellipse in an Eulerian reference frame; and, second, potential vorticity and its canonically conjugate angle, the orientation of the ellipse relative to a Lagrangian reference frame. The remaining degrees of freedom are the lengths, $a(t)$ and $b(t)$, of the two axes of the ellipse at $h = 0$. Ball's (1963) theorem on the simple harmonic oscillations of the moment of inertia, a^2+b^2, for RSW solutions suggests a transformation to plane polar coordinates given by the mean radius $r(t) = (a^2+b^2)^{\frac{1}{2}}$ and the shape parameter $\alpha(t) = \tan^{-1}(b/a)$. It turns out this transformation decouples the dynamics for the last two degrees of freedom $r(t)$ and $\alpha(t)$, thereby reducing the problem to quadrature. The key step, however, is the introduction of Lagrangian particle paths.

We choose Lagrangian coordinates which are related to the initial particle positions $\boldsymbol{x}_0$ by rescaling and re-aligning to the principle axes $(1/a_0, 1/b_0)$ of $\boldsymbol{B}(0)$, the initial value of the symmetric matrix $\boldsymbol{B}(t)$ in (2.5). Being symmetric, the matrix $\boldsymbol{B}(0)$ can be diagonalized by a 2×2 rotation matrix $\boldsymbol{R}_0$, i.e. $\boldsymbol{B}(0) = \boldsymbol{R}_0^{-1}\boldsymbol{D}_0\boldsymbol{R}_0$, with $\boldsymbol{D}_0 = \operatorname{diag}(1/a_0, 1/b_0)$. Choosing Lagrangian coordinates $\boldsymbol{l} = \boldsymbol{D}_0^{\frac{1}{2}}\boldsymbol{R}_0\boldsymbol{x}_0$ (with dimensions of [length]$^{\frac{1}{2}}$) then gives the principal axis expression $\boldsymbol{x}_0^{\mathrm{T}}\boldsymbol{B}(0)\,\boldsymbol{x}_0 = \boldsymbol{x}_0^{\mathrm{T}}\boldsymbol{R}_0^{-1}\boldsymbol{D}_0\boldsymbol{R}_0\boldsymbol{x}_0 = \boldsymbol{l}^{\mathrm{T}}\boldsymbol{l}$, which is convenient in transforming the Goldsbrough Ansatz to Lagrangian coordinates.

In terms of Lagrangian coordinates $l^a, a = 1, 2$, the elliptical-vortex solution Ansatz may now be expressed as a particle-path relation,

$$x^i(\boldsymbol{l}, t) = \boldsymbol{G}_a^i(t)\, l^a, \quad \text{with } i, a = 1, 2, \tag{2.6}$$

where $\boldsymbol{G}(t)$ (also with dimensions of [length]$^{\frac{1}{2}}$) is a time-dependent 2×2 real matrix with positive determinant. The matrix $\boldsymbol{G}(t)$ represents the time-dependent map describing the motion of a fluid particle from the rescaled and re-aligned reference position, $\boldsymbol{l}$, to the current position $\boldsymbol{x}$. It follows that

$$v^i = \left.\frac{\partial x^i}{\partial t}\right|_{\boldsymbol{l}} = (\dot{\boldsymbol{G}}\boldsymbol{G}^{-1})^i_j\, x^j. \tag{2.7}$$

We also incorporate mass conservation, expressed in the Lagrangian description as

$$h(\boldsymbol{l}, t)\det\left(\frac{\partial \boldsymbol{x}}{\partial \boldsymbol{l}}\right) = h(\boldsymbol{l}, 0)\,(a_0 b_0)^{\frac{1}{2}}. \tag{2.8}$$

Substitution into (2.5) yields the following relations for the elliptical vortex

$$\left.\begin{aligned} \boldsymbol{x} = \boldsymbol{G}(t)\,\boldsymbol{l}, \quad \boldsymbol{v} &= \dot{\boldsymbol{G}}\boldsymbol{G}^{-1}(t)\,\boldsymbol{x}, \\ h(\boldsymbol{l}, t) &= [h_0(0) - \boldsymbol{l}^{\mathrm{T}}\boldsymbol{l}]\,(a_0 b_0)^{\frac{1}{2}}/\det \boldsymbol{G}(t) \\ &= [h_0(t) - \boldsymbol{l}^{\mathrm{T}}\boldsymbol{G}^{\mathrm{T}}(t)\,\boldsymbol{B}(t)\,\boldsymbol{G}(t)\,\boldsymbol{l}]. \end{aligned}\right\} \tag{2.9}$$

Hence, the Goldsbrough elliptical-vortex variables in (2.5) may be expressed in terms of $\boldsymbol{G}(t)$, as

$$\left.\begin{aligned} h_0(t) &= \frac{h_0(0)\,(a_0 b_0)^{\frac{1}{2}}}{\det \boldsymbol{G}(t)}, \\ \boldsymbol{B}(t) &= \frac{\boldsymbol{G}^{-\mathrm{T}}(t)\,\boldsymbol{G}^{-1}(t)\,(a_0 b_0)^{\frac{1}{2}}}{\det \boldsymbol{G}(t)}, \\ \boldsymbol{A}(t) &= \dot{\boldsymbol{G}}\boldsymbol{G}^{-1}(t). \end{aligned}\right\} \tag{2.10}$$

Thus, eight Eulerian quantities (one in h_0, four in $\boldsymbol{A}$, and three in symmetric $\boldsymbol{B}$) have been replaced by eight Lagrangian quantities (four in $\boldsymbol{G}$ and four in $\dot{\boldsymbol{G}}$). Substituting (2.9) into the shallow-water equations (2.1) gives the matrix equation for $\boldsymbol{G}(t)$,

$$\ddot{\boldsymbol{G}} - f\varepsilon\dot{\boldsymbol{G}} = \frac{c\boldsymbol{G}^{-\mathrm{T}}}{\det \boldsymbol{G}}, \quad \text{with } c = 2g(a_0 b_0)^{\frac{1}{2}}, \quad \varepsilon = \begin{pmatrix} 0 & 1 \\ -1 & 0 \end{pmatrix}, \tag{2.11}$$

with initial values $\boldsymbol{G}(0) = (\boldsymbol{D}_0^{\frac{1}{2}}\boldsymbol{R}_0)^{-1}$ (so that $\det \boldsymbol{G}(0) = (a_0 b_0)^{\frac{1}{2}}$) and $\dot{\boldsymbol{G}}(0) = \boldsymbol{A}(0)\,\boldsymbol{G}(0)$. Since (2.11) is scale-invariant under $\boldsymbol{G} \to \lambda\boldsymbol{G}$ and $c \to \lambda^4 c$, the magnitudes of all the initial values can be adsorbed into the parameter c, which also contains the reduced gravity. This simply reflects the scale-symmetry of the original RSW equations. (Typical values of the parameters in (2.11) for oceanographic applications are (Young 1986): $f \approx 10^{-4}\ \mathrm{s}^{-1}$, $g \approx 1\ \mathrm{cm\ s}^{-2}$, $c \approx 4 \times 10^5\ \mathrm{cm}^2\ \mathrm{s}^{-2}$.) The eighth-order dynamical system (2.11) will be the subject of the remainder of our investigation.

3. Action principle and Hamiltonian formulation

The dynamical equation (2.11) for $\boldsymbol{G}(t)$ arises from an action principle using the following Lagrangian:

$$L = \tfrac{1}{2}\mathrm{Tr}\,(\dot{\boldsymbol{G}}^{\mathrm{T}}\dot{\boldsymbol{G}}) - f\,\mathrm{Tr}\,(\dot{\boldsymbol{G}}^{\mathrm{T}}\varepsilon\boldsymbol{G}) - \frac{c}{\det \boldsymbol{G}}. \tag{3.1}$$

Thus, the momentum canonically conjugate to $\boldsymbol{G}$ is

$$\boldsymbol{\Pi} = \frac{\partial L}{\partial \dot{\boldsymbol{G}}} = \dot{\boldsymbol{G}} - f\varepsilon\boldsymbol{G} \tag{3.2}$$

and the Hamiltonian $H(\boldsymbol{\Pi}, \boldsymbol{G})$ is found by Legendre transformation to be

$$H = \tfrac{1}{2}\mathrm{Tr}\,[(\boldsymbol{\Pi} + f\varepsilon\boldsymbol{G})^{\mathrm{T}}(\boldsymbol{\Pi} + f\varepsilon\boldsymbol{G})] + \frac{c}{\det \boldsymbol{G}}. \tag{3.3}$$

The motion equation (2.11) then reappears in canonical Hamiltonian form as

$$\dot{\boldsymbol{G}} = \frac{\partial H}{\partial \boldsymbol{\Pi}} = \boldsymbol{\Pi} + f\varepsilon\boldsymbol{G}, \quad \dot{\boldsymbol{\Pi}} = -\frac{\partial H}{\partial \boldsymbol{G}} = \frac{c}{\det \boldsymbol{G}}\boldsymbol{G}^{-\mathrm{T}}. \tag{3.4}$$

The Lagrangian L in (3.1) in invariant under two rotational symmetries,

$$\boldsymbol{G} \rightarrow \boldsymbol{G}' = \boldsymbol{O}_1 \boldsymbol{G} \boldsymbol{O}_2, \tag{3.5}$$

where $\boldsymbol{O}_1$ and $\boldsymbol{O}_2$ are 2×2 orthogonal matrices (rotations of the plane). From the relation $\boldsymbol{x}' := \boldsymbol{O}_1 \boldsymbol{x} = (\boldsymbol{O}_1 \boldsymbol{G} \boldsymbol{O}_2)(\boldsymbol{O}_2^{-1} \boldsymbol{l}) =: \boldsymbol{G}'\boldsymbol{l}'$, one sees that symmetry under $\boldsymbol{G} \rightarrow \boldsymbol{G}'$ means invariance under rotations of the Eulerian coordinates (x_1, x_2) by $\boldsymbol{O}_1$, as well as invariance under rotations of the Lagrangian coordinates (l_1, l_2) by $\boldsymbol{O}_2^{-1}$. Corresponding to these two symmetries of the Lagrangian, Noether's theorem implies two constants of motion, namely,

$$\varepsilon P_\theta = \boldsymbol{\Pi}\boldsymbol{G}^{\mathrm{T}} - \boldsymbol{G}\boldsymbol{\Pi}^{\mathrm{T}} = \dot{\boldsymbol{G}}\boldsymbol{G}^{\mathrm{T}} - \boldsymbol{G}\dot{\boldsymbol{G}}^{\mathrm{T}} - f\varepsilon\,\mathrm{Tr}\,(\boldsymbol{G}^{\mathrm{T}}\boldsymbol{G}), \tag{3.6}$$

from $\boldsymbol{O}_1$ (left invariance) and

$$\varepsilon P_\phi = \boldsymbol{\Pi}^{\mathrm{T}}\boldsymbol{G} - \boldsymbol{G}^{\mathrm{T}}\boldsymbol{\Pi} = \dot{\boldsymbol{G}}^{\mathrm{T}}\boldsymbol{G} - \boldsymbol{G}^{\mathrm{T}}\dot{\boldsymbol{G}} + 2f\varepsilon(\det \boldsymbol{G}), \tag{3.7}$$

from $\boldsymbol{O}_2$ (right invariance). Physically, P_θ is the angular momentum coming from invariance under rotations of Eulerian reference coordinates, and P_ϕ is the potential vorticity (integrated over the ellipse) coming from invariance under rotations of the Lagrangian coordinate axes (relabelling of fluid particles). Both P_θ and P_ϕ may be verified to be constants directly from the equation of motion for $\boldsymbol{G}$.

The Lagrangian (3.1) is also invariant under the discrete symmetry $\boldsymbol{G} \leftrightarrow \boldsymbol{G}^{\mathrm{T}}$, which reverses the roles and senses of Eulerian and Lagrangian rotations, and interchanges the angular momentum and the potential vorticity, $P_\theta \leftrightarrow P_\phi$. This discrete symmetry is the Dedekind duality principle for elliptical-vortex solutions of the RSW equations. This duality principle exchanges, for example, an elliptical-vortex solution which is uniformly rotating for its dual solution whose boundary is fixed, yet contains swirling flow. For self-gravitating figures of equilibrium the Dedekind duality principle interchanges Jacobi and Dedekind ellipsoids. (See Chandrasekhar 1969 for further discussion of Dedekind duality in the context of self-gravitating figures of equilibrium.) This reversal of the roles and senses of Eulerian and Lagrangian rotations corresponds to reversing spaced-fixed, and body-fixed coordinates in the dynamics of a rigid body.

4. Hamiltonian reduction and solution by quadrature

To reduce the system to its essential elements, we isolate the angles conjugate to P_θ and P_ϕ by expressing $\boldsymbol{G}$ (via the polar decomposition) as

$$\boldsymbol{G} = \boldsymbol{R}_1 \boldsymbol{D} \boldsymbol{R}_2, \tag{4.1}$$

where $\boldsymbol{R}_1$ and $\boldsymbol{R}_2$ are 2×2 rotation matrices and $\boldsymbol{D}$ is diagonal. That is,

$$\boldsymbol{G} = \begin{pmatrix} \cos\theta & \sin\theta \\ -\sin\theta & \cos\theta \end{pmatrix} \begin{pmatrix} a & 0 \\ 0 & b \end{pmatrix} \begin{pmatrix} \cos\phi & \sin\phi \\ -\sin\phi & \cos\phi \end{pmatrix}. \tag{4.2}$$

The matrix $\boldsymbol{R}_1(\theta)$ describes the orientation of the boundary of the ellipse relative to a fixed Eulerian reference frame, and $\boldsymbol{R}_2(\phi)$ describes the orientation of a line of fluid particles, swirling inside the ellipse, relative to a Lagrangian reference frame aligned with the principal axes of the symmetric matrix $\boldsymbol{B}(0)$. The diagonal matrix $\boldsymbol{D}$ describes the (strictly positive) lengths of its two axes, thereby determining the shape and area of the elliptical vortex. (Interchanging a and b corresponds to an inessential reorientation of the ellipse by $\frac{1}{2}\pi$.) The polar decomposition of $\boldsymbol{G}$ clearly shows the reversal of Eulerian and Lagrangian rotations under $\boldsymbol{G} \leftrightarrow \boldsymbol{G}^{\mathrm{T}}$.

Upon defining angular frequencies

$$\omega_1 = -\boldsymbol{R}_1^{-1}\dot{\boldsymbol{R}}_1 = -\dot{\theta}\varepsilon \quad \text{and} \quad \omega_2 = -\dot{\boldsymbol{R}}_2\boldsymbol{R}_2^{-1} = -\dot{\phi}\varepsilon, \tag{4.3}$$

we may express the previous conserved quantities as

$$\varepsilon P_\theta = \boldsymbol{R}_1(2\boldsymbol{D}\omega_2\boldsymbol{D} - \boldsymbol{D}^2\omega_1 - \omega_1\boldsymbol{D}^2)\boldsymbol{R}_1^{-1} - f(\mathrm{Tr}\,\boldsymbol{D}^2)\,\varepsilon = [2ab\dot{\phi} - (a^2+b^2)(f-\dot{\theta})]\,\varepsilon, \tag{4.4a}$$

$$\varepsilon P_\phi = \boldsymbol{R}_2(\boldsymbol{D}^2\omega_2 + \omega_2\boldsymbol{D}^2 - 2\boldsymbol{D}\omega_1\boldsymbol{D})\boldsymbol{R}_2^{-1} - 2f(\det\boldsymbol{D})\,\varepsilon = [(a^2+b^2)\,\dot{\phi} - 2ab(f-\dot{\theta})]\,\boldsymbol{\varepsilon}. \tag{4.4b}$$

Here we have used $[\boldsymbol{R}_1, \varepsilon] = 0 = [\boldsymbol{R}_2, \varepsilon]$. These constants of motion demonstrate the coupling in the elliptical-vortex flows among rotation, swirl and deformation. Note that $P_\theta \leftrightarrow P_\phi$ under $(f-\dot{\theta}) \leftrightarrow \dot{\phi}$, reflecting the Dedekind duality in the angular variables explicitly.

Substituting the polar decomposition $\boldsymbol{G} = \boldsymbol{R}_1\boldsymbol{D}\boldsymbol{R}_2$ into the Lagrangian (3.1) gives

$$L = \tfrac{1}{2}\dot{a}^2 + \tfrac{1}{2}\dot{b}^2 + \tfrac{1}{2}(a^2+b^2)\,\dot{\theta}^2 + \tfrac{1}{2}(a^2+b^2)\,\dot{\phi}^2 + 2ab\dot{\theta}\dot{\phi} - f(a^2+b^2)\,\dot{\theta} - 2fab\dot{\phi} - \frac{c}{ab}. \tag{4.5}$$

As a check, notice that the Lagrangian is independent of the angles θ and ϕ, leading to conservation of their canonical momenta,

$$P_\theta = \frac{\partial L}{\partial \dot{\theta}} = 2ab\dot{\phi} - (a^2+b^2)(f-\dot{\theta}), \tag{4.6a}$$

$$P_\phi = \frac{\partial L}{\partial \dot{\phi}} = (a^2+b^2)\,\dot{\phi} - 2ab(f-\dot{\theta}). \tag{4.6b}$$

Not unexpectedly, this agrees with the earlier calculations in (4.4*a*, *b*).

We now pass to the Hamiltonian description in the polar decomposition variables via the usual Legendre transformation. Namely,

$$H = p\dot{q}-L = \tfrac{1}{2}P_a^2+\tfrac{1}{2}P_b^2+\tfrac{1}{2}(a^2+b^2)(\dot{\theta}^2+\dot{\phi}^2)+2ab\dot{\theta}\dot{\phi}+\frac{c}{ab}. \tag{4.7}$$

Hence, we have (in a form reminiscent of Riemann's 1860 formula (7.2))

$$H = \tfrac{1}{2}P_a^2+\tfrac{1}{2}P_b^2+\frac{(P_\theta+P_\phi)^2}{4(a+b)^2}+\frac{(P_\theta-P_\phi)^2}{4(a-b)^2}+fP_\theta+\tfrac{1}{2}f^2(a^2+b^2)+\frac{c}{ab}, \tag{4.8}$$

where P_a and P_b are momenta canonically conjugate to a and b, respectively, and the quantities $\dot{\theta}$ and $\dot{\phi}$ have been evaluated by using expressions (4.6) for the constants of motion P_θ and P_ϕ,

$$\dot{\theta} = \frac{(P_\theta+P_\phi)}{2(a+b)^2}+\frac{(P_\theta-P_\phi)}{2(a-b)^2}+f = \frac{\partial H}{\partial P_\theta}, \tag{4.9a}$$

$$\dot{\phi} = \frac{(P_\theta+P_\phi)}{2(a+b)^2}-\frac{(P_\theta-P_\phi)}{2(a-b)^2} = \frac{\partial H}{\partial P_\theta}. \tag{4.9b}$$

Once the deformation dynamics is known for the elliptical axes $a(t)$ and $b(t)$, the angular evolution for $\theta(t)$, the Eulerian orientation of the elliptical boundary, and $\phi(t)$, the Lagrangian orientation of a line of fluid particles within the ellipse, may be obtained from (4.9*a*, *b*) by quadratures.

Hamilton's equations for the axes of the ellipse are given by

$$\dot{a} = \frac{\partial H}{\partial P_a} = P_a, \quad \dot{b} = \frac{\partial H}{\partial P_b} = P_b, \tag{4.10a}$$

$$\dot{P}_a = -\frac{\partial H}{\partial a} = -\frac{\partial V}{\partial a}, \quad \dot{P}_b = -\frac{\partial H}{\partial b} = -\frac{\partial V}{\partial b}, \tag{4.10b}$$

where

$$\begin{aligned} V &= \tfrac{1}{2}(a^2+b^2)(\dot{\theta}^2+\dot{\phi}^2)+2ab\dot{\theta}\dot{\phi}+\frac{c}{ab} \\ &= \frac{(P_\theta+P_\phi)^2}{4(a+b)^2}+\frac{(P_\theta-P_\phi)^2}{4(a-b)^2}+\tfrac{1}{2}f^2(a^2+b^2)+\frac{c}{ab}. \end{aligned} \tag{4.11}$$

Thus, the problem is reduced to nonlinear oscillations with two degrees of freedom ($a(t)$ and $b(t)$, the two axes of the ellipse) followed by the quadratures in (4.9*a*, *b*) to reconstruct the full solution.

To proceed farther, we transform Hamilton's equations (4.10*a*, *b*) from Cartesian to polar coordinates and take advantage of Ball's (1963) theorem on the simple harmonic oscillations of the moment of inertia of *all* RSW flows, including the elliptical-vortex flows. In polar coordinates,

$$\left.\begin{aligned} r &= (a^2+b^2)^{\frac{1}{2}}, & a &= r\cos\alpha, \\ \alpha &= \tan^{-1}(b/a), & b &= r\sin\alpha, \end{aligned}\right\} \tag{4.12}$$

one computes

$$ab = r^2\sin\alpha\cos\alpha = \tfrac{1}{2}r^2\sin 2\alpha, \tag{4.13}$$

$$(a\pm b)^2 = a^2+b^2\pm 2ab = r^2(1\pm\sin 2\alpha), \tag{4.14}$$

$$P_a^2+P_b^2 = P_r^2+\frac{P_\alpha^2}{r^2}. \tag{4.15}$$

Thus, the Hamiltonian in polar coordinates (r, α) becomes

$$H = fP_\theta + \tfrac{1}{2}(P_r^2 + f^2 r^2) + \frac{1}{r^2} K(\alpha, P_\alpha), \tag{4.16}$$

where
$$K(\alpha, P_\alpha) = \tfrac{1}{2}P_\alpha^2 + V(\alpha), \tag{4.17}$$

with
$$V(\alpha) = \frac{(P_\theta + P_\phi)^2}{4(1+\sin 2\alpha)} + \frac{(P_\theta - P_\phi)^2}{4(1-\sin 2\alpha)} + \frac{2c}{\sin 2\alpha}. \tag{4.18}$$

The first term in H in (4.16) generates a rotation in θ at the inertial frequency f, taking the system into the rotating frame of the f-plane. The second term generates simple-harmonic radial oscillations at the inertial frequency. The last term (the piece involving the elliptical aspect ratio, $\tan\alpha$), is homogeneous in r of degree -2. This homogeneity allows an immediate separation between the dynamics of r and α, as follows. Hamilton's equations imply

$$\frac{d^2}{dt^2} r^2 = 2\left(\dot{r}^2 - r\frac{\partial H}{\partial r}\right) = 2\left(P_r^2 - r\frac{\partial H}{\partial r}\right) = -4f^2 r^2 + 4(H - fP_\theta). \tag{4.19}$$

Thus, since H and P_θ are constants in (4.19), the sum of the squares of the elliptical axes lengths (i.e. the moment of inertia) undergoes simple harmonic motion around its initial value with frequency $2f$ (i.e. at *twice* the inertial frequency). That is,

$$r^2(t) = r_0^2 + A\cos(2ft) + B\sin(2ft) \tag{4.20}$$

where
$$r_0^2 = (H - fP_\theta)/f^2, \quad A = r^2(0) - r_0^2, \quad B = \frac{dr^2}{dt}(0)/2f.$$

The first integral of (4.19) for the dynamics of the sum of squares of the elliptical axes is related to the Hamiltonian for the dynamics of the elliptical aspect ratio, α, by

$$\begin{aligned} \text{const} &= \frac{1}{2}\left(\frac{dr^2}{dt}\right)^2 - 4(H - fP_\theta)r^2 + 2f^2 r^4 \\ &= 4r^2[\tfrac{1}{2}(P_r^2 + f^2 r^2) - (H - fP_\theta)] \\ &= -4K(\alpha, P_\alpha). \end{aligned} \tag{4.21}$$

Hence, $K(\alpha, P_\alpha)$ is a *constant of motion* and the last term in the Hamiltonian in (4.16) may be regarded as a generalized angular-momentum potential. The α-dynamics follows from Hamilton's equations,

$$\frac{d\alpha}{dt} = \frac{\partial H}{\partial P_\alpha} = \frac{1}{r^2(t)}\frac{\partial K}{\partial P_\alpha}, \tag{4.22}$$

$$\frac{dP_\alpha}{dt} = -\frac{\partial H}{\partial \alpha} = \frac{-1}{r^2(t)}\frac{\partial K}{\partial \alpha}. \tag{4.23}$$

Thus, the conserved quantity $K(\alpha, P_\alpha)$ may be interpreted as the Hamiltonian for the aspect-ratio dynamics of α in terms of a rescaled time, τ, defined by $d\tau = dt/r^2(t)$. In terms of τ we have the canonical equations,

$$\frac{d\alpha}{d\tau} = \frac{\partial K}{\partial P_\alpha}, \quad \frac{dP_\alpha}{d\tau} = -\frac{\partial K}{\partial \alpha}, \tag{4.24}$$

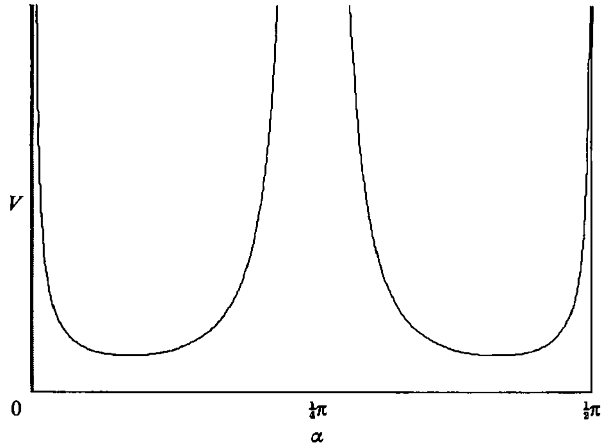

FIGURE 1. The aspect-ratio potential $V(\alpha)$ for $P_\theta \neq P_\phi$. In this case, the axisymmetric state, $\alpha = \frac{1}{4}\pi$, is singular.

or, in Newtonian form,

$$\frac{\mathrm{d}^2\alpha}{\mathrm{d}\tau^2} = -\frac{\mathrm{d}V(\alpha)}{\mathrm{d}\alpha}, \quad \text{with} \quad V(\alpha) = \left[\frac{(P_\theta + P_\phi)^2}{4(1+\sin 2\alpha)} + \frac{(P_\theta - P_\phi)^2}{4(1-\sin 2\alpha)} + \frac{2c}{\sin 2\alpha}\right], \tag{4.25}$$

leading in the usual way to a closed-form (implicit) solution for $\tau(\alpha)$ in terms of elliptic integrals. Actually evaluating the elliptical integrals is unnecessary, though, because the dynamical behaviour of the aspect ratio for the elliptic-vortex solutions can be read off from the graphs of the potential $V(\alpha)$ plotted in figure 1 and figure 2. As shown in figure 1 for $P_\theta \neq P_\phi$, at finite energy K, the quantity α oscillates in the scaled time variable, τ, and is confined within one of two physically equivalent sectors, either in $(0, \frac{1}{4}\pi)$ (i.e. $a < b$), or in $(\frac{1}{4}\pi, \frac{1}{2}\pi)$ (i.e. $a > b$). The two sectors differ only by the exchange of a and b, equivalent to a rotation in θ by $\frac{1}{2}\pi$. Yet for $P_\theta \neq P_\phi$, there is an 'angular-momentum barrier' in the potential $V(\alpha)$ at $\alpha = \frac{1}{4}\pi$, which prevents one sector with $a \neq b$ being reached from the other one by passing through $a = b$, the axisymmetric state. Thus, for $P_\theta \neq P_\phi$, the axisymmetric state is a singular point of the aspect-ratio potential and cannot be reached. (This is analogous to the exclusion of collision orbits leading to $r = 0$ in the Kepler problem for non-zero angular momentum.)

In each of the two sectors shown in figure 1 for $P_\theta \neq P_\phi$ the potential $V(\alpha)$ has only one minimum, so α performs periodic oscillations in τ around that minimum. Because $r^2(t)$ is positive, equilibria in the scaled time variable, τ, are also equilibria in normal time, t. These equilibria occur at the minima of $V(\alpha)$ for $P_\alpha = 0$. For example, the rodon solution has $P_\alpha = 0 = P_r$ and $r^2(t) = r_0^2$, so it is an equilibrium in both α and r. Its rotation in the Eulerian frame, and its internal motion are determined from the quadrature formulae (4.9*a*) and (4.9*b*). The pulsrodon solution of Rogers (1989), rotates and pulses periodically with parameters $P_\phi = 0$, $P_r \neq 0$, $P_\alpha \neq 0$, and is simple-harmonic in $r^2(t)$ with $P_\theta \neq 0$. Note that the discrete symmetry (3.8) leads to an additional solution, dual to the pulsrodon under $P_\theta \leftrightarrow P_\phi$. This dual solution pulses and has internal motion (periodic swirling of Lagrangian particles such that all particles have the same period), and the Eulerian orientation of the axes of its (instantaneous) elliptical boundary is determined from its internal motion by the

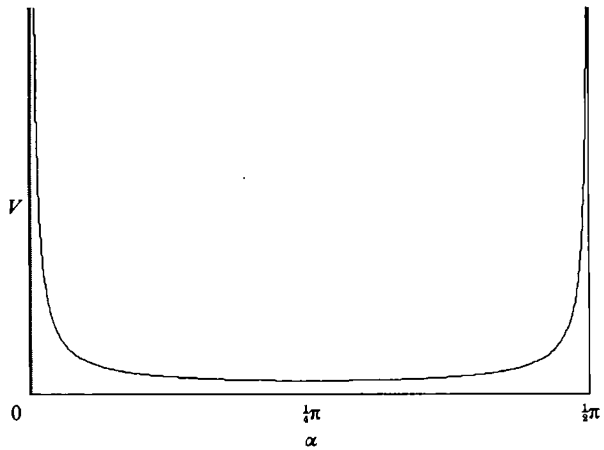

FIGURE 2. The aspect-ratio potential $V(\alpha)$ for $P_\theta \neq P_\phi$. In this case, the axisymmetric state, $\alpha = \frac{1}{4}\pi$, is regular and stable.

quadrature (4.9). In general, solutions with $P_\theta \neq P_\phi$ and both P_θ and P_ϕ non-zero will swirl, pulse, and rotate quasi-periodically, leading to the beautiful Lissajous-type figures seen numerically in the Appendix to this paper by David & Ohsumi. All of these solutions are orbitally Lyapunov stable to perturbations in the space of elliptical-vortex solutions (i.e. they are Lyapunov stable to changes of initial conditions, modulo rotations by θ and ϕ).

When $P_\theta = P_\phi$ the singularity in $V(\alpha)$ at $\alpha = \frac{1}{4}\pi$ is absent, as shown in figure 2. In fact, for this special case $V(\alpha)$ has a minimum at $\alpha = \frac{1}{4}\pi$, the axisymmetric case. So the axisymmetric solution exists when $P_\theta = P_\phi$, and nearby elliptical solutions will undergo oscillations through the axisymmetric state from one sector (say, $a < b$) to the other ($a > b$) without hindrance. Thus, the axisymmetric solutions are stable (i.e. $V(\alpha)$ has a minimum) in the class of elliptical-vortex solutions for perturbations that preserve the relation $P_\theta = P_\phi$. Perturbations that break the relation $P_\theta = P_\phi$ lead to oscillating elliptical solutions which stay near the axisymmetric state but remain confined within the sector, ($a < b$) or ($a > b$), in which they start initially. Thus, the axisymmetric solution is also orbitally Lyapunov stable to perturbations in the class of elliptical-vortex solutions.

5. Summary

The present analysis uses methods from Hamiltonian mechanics to prove that the elliptical-vortex solutions are quasi-periodic and integrable. Of the eight dimensions in the solution, four are in action-angle pairs (θ, P_θ; ϕ, P_ϕ), two are simple-harmonic ($r^2, \mathrm{d}r^2/\mathrm{d}t$), and two are periodic Newtonian oscillations (α, P_α). The general motion is reconstructed by integrating the α equation in the rescaled time variable, τ, transforming to the normal time variable, t, using the r^2 equation, then integrating out the remaining angle variables, θ and ϕ. All steps of the reconstruction are quadratures and each variable at every step has a clear physical meaning.

Remark on orbital stability and on chaotic behaviour. The analysis leading to (4.24) shows that the reduced system has only periodic solutions, with no bifurcations and no hyperbolic orbits. Thus, all equilibria – including the rodons – are orbitally stable (that is, stable modulo phase drifts in θ and ϕ), in the class of elliptical-vortex solutions. The full reconstructed solution is regular and quasiperiodic with at most four frequencies, and does not exhibit sensitive dependence on initial conditions (chaos). In particular, no chaos appears in the elliptical-vortex solutions themselves and one may expect only subharmonic resonance effects in the presence of damping and driving of the elliptical-vortex system, which might be used to mimic, say, interactions of elliptical vortices with external currents, or with additional layers.

I would like to thank D. Kirwan and C. Rogers for stimulating my interest in this problem. Some of this work was done at the University of Minnesota Institute for Mathematics and its Applications while I was a visitor there, and I am grateful for their hospitality. I would also like to thank D. David and T. Ohsumi, whose numerical work on this problem shown in the appendix convinced me the elliptical-vortex motion is not chaotic. Finally, I would like to thank J. Marsden, P. Ripa, and W. Young for their helpful comments.

Appendix. Numerical study of elliptical vortices in shallow water

By D. David[1] *and T. K. Ohsumi*[2]

[1] *Theoretical Division and Center for Nonlinear Studies, Los Alamos National Laboratory*

[2] *Physics Department, University of California, Santa Cruz*

In this Appendix, we examine numerically the behaviour of solutions in the reduced two-degree-of-freedom system (4.10) in the body of the paper. These solutions are computed using the following representation. Take

$$u = a+b, \quad v = a-b, \tag{A 1}$$

to be the sum and difference of the elliptical axes lengths. The dynamical system for $u(t)$ and $v(t)$ following from equation (4.10) is

$$\frac{\mathrm{d}^2u}{\mathrm{d}t^2} = \frac{P_\sigma^2}{u^3}+\frac{16cu}{(u^2-v^2)^2}-f^2u, \quad \frac{\mathrm{d}^2v}{\mathrm{d}t^2} = \frac{P_\tau^2}{v^3}+\frac{16cv}{(u^2-v^2)^2}-f^2v, \tag{A 2}$$

where $P_\sigma^2 = \frac{1}{2}(P_\theta+P_\phi)^2$ and $P_\tau^2 = \frac{1}{2}(P_\theta-P_\phi)^2$. In the numerical computations, we have chosen the values $f = 0.5$ for the frequency parameter and $c = 0.1$ for the reduced gravity parameter. Also, we have fixed the following initial conditions:

$$\theta+\phi = 0, \quad \theta-\phi = 1.0, \quad P_u = 0, \quad P_v = 0.1, \quad u = 2, \quad v = 1 \tag{A 3}$$

(where $P_u = \dot{a}+\dot{b}$ and $P_v = \dot{a}-\dot{b}$) and we have varied the numerical values of the constants P_σ^2 and P_τ^2. The solutions of (A 2) live on manifolds embedded in R^4 (coordinated by the four variables u, v, P_u, and P_v). The body of the paper characterizes these manifolds as four-tori. Generically, the solutions form dense coverings of the tori. However they will be closed curves on the tori whenever all the ratios of the various periods are rational numbers; for this situation, we may think of the solutions as generalizations of the well-known Lissajous figures to closed orbits in higher dimensions. The orbits actually do reduce to genuine Lissajous patterns when the parameter c vanishes; in that case, (A 2) uncouple to a set of two oscillators whose solutions for u^2 and v^2 undergo simple harmonic motion at frequency f. The pictures presented below (figures 3–6) are projections of the dynamics in R^4 onto three-dimensional subspaces for $c \neq 0$; it is therefore not surprising to see that the projections of the solutions are self-intersecting.

(a) (b)

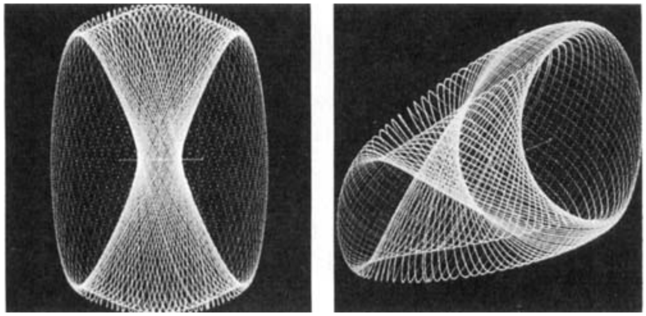

FIGURE 3. (v, P_u, P_v) projection of axisymmetric oscillations for $P_\theta = P_\phi$. (a) The viewpoint shows reflection symmetry in the (v, P_v) plane; (b) as seen from another viewpoint.

(a) (b)

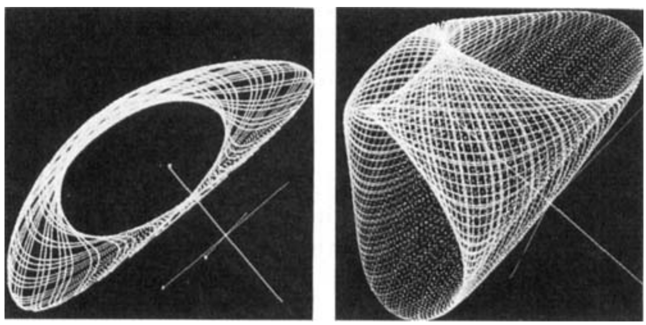

FIGURE 4. (a) (u, v, P_v) projection of elliptical vortex motion for $P_\theta = -P_\phi$. (b) (v, P_u, P_v) projection of elliptical vortex motion for $P_\theta = -P_\phi$.

The first example is characterized by the choice $P_\tau^2 = 0$ and $P_\sigma^2 = 1.0$. Now $P_\tau = 0$ implies that $P_\theta = P_\phi$. In this case, the physically relevant region of the α (aspect ratio) phase plane is the full sector $(0, \frac{1}{2}\pi)$ rather than the union of the disconnected angular intervals $(0, \frac{1}{4}\pi)$ and $(\frac{1}{4}\pi, \frac{1}{2}\pi)$. Figure 3(a) shows the projection of the solution in the (v, P_u, P_v) subspace viewed from above the (P_v, v) plane; figure 3(b) shows the same solution, using a different line of sight. In figure 3(a), we notice a mirror symmetry with respect to the variable v. This reflects the interchange symmetry for aspect ratios a/b and b/a of the ellipse (in other words, invariance under the interchange of the semi-major and semi-minor axes of the ellipse).

Figures 4(a) and 4(b) depict solutions for the choice $P_\tau^2 = 1.0$ and $P_\sigma^2 = 0$. Here, $P_\sigma = 0$ implies $P_\theta = -P_\phi$, which means that the rotating and swirling components of the dynamics proceed in opposite directions. The pulsing effect mentioned in the body of the paper is shown here; the orbits undergo oscillations with amplitudes that increase and decrease alternately. Not unexpectedly, the mirror symmetry pointed out in the preceding paragraph also occurs for this case. Figure 4(a) presents the solution in the (u, v, P_v) subspace. This projection is transverse to one of the toroidal components of the topology of the orbit; so a hole appears in the picture. (Holes are observed for all numerically computed orbits; however, they are obvious only in particular projections.) Figure 4(b) shows the same solution, but projected in the (v, P_u, P_v) subspace.

(a) (b)

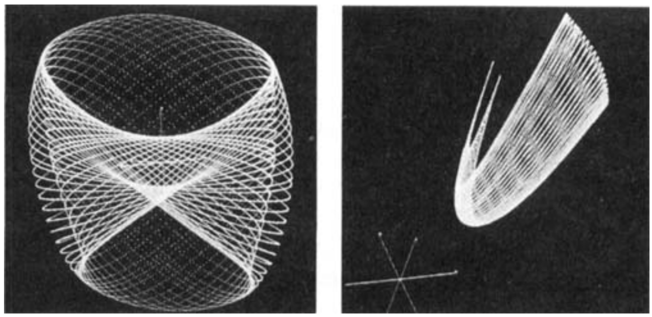

FIGURE 5. (a) (v, P_u, P_v) projection of elliptical vortex motion for $P_\theta = 0 = P_\phi$. (b) Elliptical vortex motion for $P_\theta = 0 = P_\phi$, plotting (u, v) versus the potential V in (A 4).

(a) (b) (c)

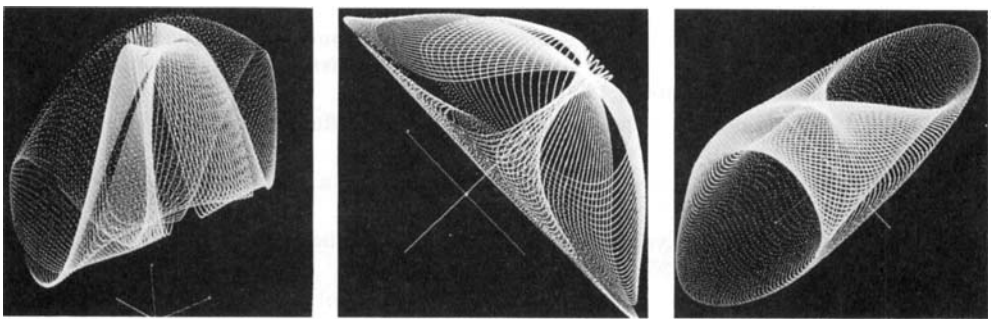

FIGURE 6. (a) (u, P_v, V), (b) (u, v, P_v), and (c) (v, P_u, P_v) projections for $P_\tau = 0.1$ and $P_\sigma = 0.2$.

Figures 5(a) and 5(b) exemplify a solution with $P_\tau^2 = P_\sigma^2 = 0$. Figure 5(a) shows the solution in the (v, P_u, P_v) subspace. Figure 5(b) gives another representation of the solution, this time by plotting it on the potential surface $V(u, v)$, given in (4.11) in the text, and in these variables,

$$V(u, v) = \frac{P_\sigma^2}{4u^2} + \frac{P_\tau^2}{4v^2} + \tfrac{1}{4}f^2(u^2+v^2) + \frac{4c}{u^2v^2}. \tag{A 4}$$

That is, the solution is shown in the space (u, v, V); where the orbit sweeps the potential surface in a regular way. This representation of the solution is analogous to a ball rolling under gravity on the surface $V(u, v) =$ constant.

When both of the angular momenta P_τ and P_σ are non-zero, the motion involves slightly more complicated patterns than in the case when one of the angular momenta vanishes. This is shown in figure 6(a), which depicts the solution for the choice $P_\tau = 0.1$ and $P_\sigma = 0.2$ in the space (v, P_v, V); the behaviour for both P_τ and P_σ non-zero exhibits more complex patterns of sweeping (e.g. compare figures 5a and 6c). Figures 6(b) and 6(c) show the same orbit in the (u, v, P_v) subspace and the (v, P_u, P_v) subspace, respectively.

REFERENCES

BALL, F. K. 1963 Some general theorems concerning the finite motion of a shallow liquid lying on a paraboloid. *J. Fluid Mech.* **17**, 240–256.

Ball, F. K. 1965 The effect of rotation on the simpler modes of motion of a liquid in an elliptic paraboloid. *J. Fluid Mech.* **22**, 529–545.

Basset, A. B. 1880 *A Treatise on Hydrodynamics*, vol. II Chap. XV. Cambridge: Deighton-Bell. (Reprinted by Dover 1961.)

Chandrasekhar, S. 1969 *Ellipsoidal Figures of Equilibrium*. Yale University Press.

Cushman-Roisin, B. 1987 Exact analytical solutions for elliptical vortices of the shallow-water equations. *Tellus* **39A**, 235–244.

Cushman-Roisin, B., Heil, W. H. & Nof, D. 1985 Oscillations and rotations of elliptical warm-core rings. *J. Geophys. Res.* **90**, 11756–11764.

Dedekind, R. 1860 Zusatz zu der vorstehenden Abhandlung. *J. Reine Angew. Math.* **58**, 217–228.

Dirichlet, G. L. 1860 Untersuchungen über ein Problem der Hydrodynamik. *J. Reine Angew. Math.* **58**, 181–216.

Dyson, F. J. 1968 Dynamics of a spinning gas cloud. *J. Math. Mech.* **18**, 91–101.

Goldsbrough, G. R. 1930 The tidal oscillations in an elliptic basin of variable depth. *Proc. R. Soc. Lond.* A **130**, 157–167.

Greenhill, A. G. 1879 On the rotation of a liquid ellipsoid about its mean axis. *Proc. Camb. Phil. Soc.* **3**, 233–246.

Holm, D. D. 1982 Gyroscopic analog for magnetohydrodynamics. In *Mathematical Methods in Hydrodynamics and Integrability in Related Dynamical Systems* (ed. M. Tabor & Y. Treve), pp. 73–84. American Institute of Physics.

Holm, D. D. 1983 Magnetic tornadoes: three-dimensional affine motions in ideal magnetohydrodyamics. *Physica* D **8**, 170–182.

Holm, D. D. 1986 Gyroscopic analog for collective motion of a stratified fluid. *J. Math. Anal. Appl.* **117**, 57–80.

Holm, D. D. & Long, B. 1989 Lyapunov stability of ideal stratified fluid equilibria in hydrostatic balance. *Nonlinearity* **2**, 23–35.

Kirchhoff, G. 1876 *Vorlesungen über Mathematische Physik*, vol. 1. Leipzig: Teubner.

Kirwan, A. D. & Liu, J. 1991 The shallow water equations on an F plane. In *Proc. Intl School of Physics Enrico Fermi, Varenna, Italy.*

Lamb, H. 1932 *Hydrodynamics*. Cambridge University Press. (Reprinted by Dover 1945.)

Riemann, B. 1860 Untersuchungen über die Bewegung eines flüssigen gleichartigen Ellipsoides. *Abh. d. Königl. Gesell. der Wis. zu Göttingen* **9**, 3–36.

Ripa, P. 1987 On the stability of elliptical vortex solutions of the shallow-water equations. *J. Fluid Mech.* **183**, 343–363.

Rogers, C. 1989 Elliptic warm-core theory: the pulsrodon. *Phys. Lett.* A **138**, 267–273.

Rogers, C. & Ames, W. F. 1989 *Nonlinear Boundary Value Problems in Science and Engineering*, §4.12. Academic.

Thacker, W. C. 1981 Some exact solutions to the nonlinear shallow water wave equations. *J. Fluid Mech.* **107**, 499–508.

Young, W. R. 1986 Elliptical vortices in shallow water. *J. Fluid Mech.* **171**, 101–119.